Comparison of the Response of a 9kW-Class Hall Effect Thruster to Facility Pressure Between Two Test Facilities

IEPC-2025-708

Presented at the 39th International Electric Propulsion Conference, Imperial College London, London, United Kingdom
14-19 September 2025

Madison G. Allen*[1], Janice Cabrera[2], Naia Butler-Craig[2], William Hurley[1], Ari Eckhaus[1], Mitchell Walker[2], and Benjamin Jorns[1]

[1] *University of Michigan, Ann Arbor, MI, USA 48103*
[2] *Georgia Institute of Technology, Atlanta, GA, USA 30332*

A pressure study is performed on a 9 kW-class Hall effect thruster at the Georgia Institute of Technology Vacuum Testing Facility 2 and the University of Michigan Large Vacuum Testing Facility at the same thruster operating condition of 4.5 kW and 300 V discharge voltage. The study was conducted to compare the performance and plume behavior across facilities and extrapolate from VTF-2 to LVTF with its 1.6x higher pumping speed. It was found that the global performance metrics were independent of pressure at VTF-2 but pressure-dependent at LVTF. Both facilities demonstrated similar pressure dependencies for the plume measurements, but they did not agree across facilities. The differences are discussed in relation to the possibility there are gradients in pressure that differ across facilities. These findings offer insights into the variability of thruster performance across facilities.

I. Introduction

The challenge of ground testing is one of the major obstacles for the development and qualification of Hall effect thrusters. This problem stems in large part from the fact that the limited pumping speed of ground test facilities results in background pressures that are orders of magnitude greater than the on-orbit environment. This high density of neutrals produces a variety of pressure-related facility effects. Notable examples include impacts on thrust, plume divergence, and plume oscillations.[1–9]

In light of this testing challenge, it has become an increasingly common practice to attempt to extrapolate data from parametric tests as a function of facility pressure to low-pressure, on-orbit conditions.[2,4,6,9] The fidelity of this process is ultimately a function of the diversity of data and the validity of the underlying model that is used to perform the extrapolation. The NASA-sponsored Joint Advanced Propulsion Institute (JANUS) has been attempting to address both of these technical challenges by developing improved probing techniques and models based on advanced forms of probabilistic data regression.[10] With that said, absent detailed experimental data from orbit, there are at present limited ways to verify the extrapolative capability of the tools and techniques developed under this institute. As an intermediate step, JANUS has focused in the past year on demonstrating the ability to extrapolate between two disparate ground test facilities. The goal of this work is to present and analyze the results from this experimental campaign, the Facility Interpolation Test (FIT), to generate these datasets.

This paper is organized in the following way. In Section 2, we first present the methods of this study including background on the thruster, facilities, and diagnostics. We then present the results of the performance and plume properties at various background pressures, in Section 3. In Section 4, we discuss our findings with the goal of proposing explanations for differences exhibited between the tests.

*Ph.D. Candidate, Aerospace Engineering, mgallen@umich.edu

II. Methods

The purpose of the FIT test is to first demonstrate similar performance and behavior at two facilities. The second is to be able to extrapolate performance and plume measurements with respect to pressure from one facility to another with slightly lower pressure. For this task, we performed a pressure study on the same test article, an H9 Hall effect thruster, at the Georgia Institute of Technology's Vacuum Testing Facility 2 (VTF-2) for the FIT 1 campaign. We replicated the study at the University of Michigan's Large Vacuum Testing Facility (LVTF) in the FIT 2 campaign. In this section, we present the test article as well as the test facilities. We also provide descriptions of the diagnostics we used to measure plume properties and performance.

A. Test Article

The H9 is a 9kW class, magnetically-shielded Hall effect thruster with a center-mounted cathode created jointly by the NASA Jet Propulsion Laboratory, the Air Force Research Laboratory, and the University of Michigan (Fig. 1).[11,12] The thruster is nominally designed for xenon, but for this study, we operated the thruster at 4.5kW 300V on krypton with a 7% cathode flow fraction. For this campaign experiment, we tested the same thruster at both facilities and with the same floating-body electrical configuration. We note that we did use a different cathode between tests, though it was of the same model. We operated the thruster at constant power (300 V discharge voltage and 4.5 kW power) while varying background pressures during this campaign.

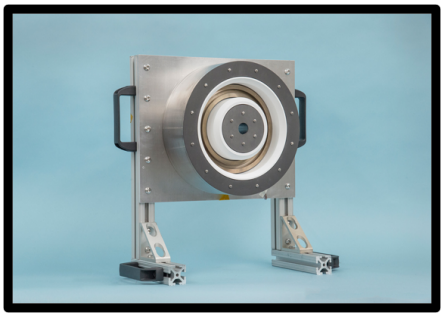

Figure 1: An image of the H9 Hall effect thruster

B. Testing Facilities

We show the schematic of both facilities in Fig. 2 and discuss their configuration in the following sections.

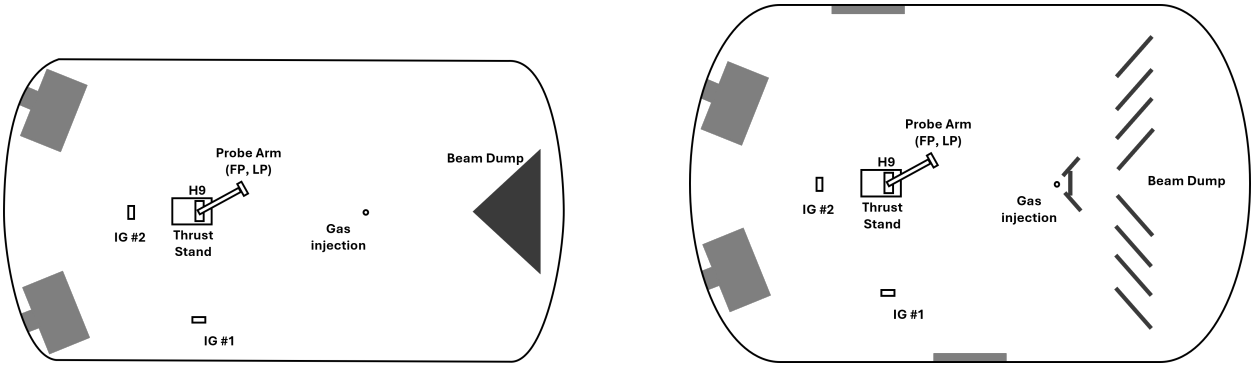

Figure 2: Schematics of a.)VTF-2 and b.) LVTF

1. VTF-2

The Georgia Institute of Technology Vacumm Testing Facility 2 (VTF-2) (Fig. 2a) is a 9.2m x 4.9m vacuum testing facility. It holds 10 PHPK TM1200i He cryopumps shielded by LN2 cooled shrouds. During the FIT 1 test, the minimum background pressure was 2.5E-7 Torr-Kr. The beam dump in this facility is oriented in a conical shape with graphite slats.

2. LVTF

The University of Michigan's Large Vacuum Testing Facility (LVTF) (Fig. 2b) is a 9m x 6m chamber with 18 cryopumps. There are 13 PHPK TM1200i He cryopumps with LN2-cooled shrouds and 6 additional PEPL He pumps that were not LN2 cooled. During this campaign, 12 PHPK and 4 PEPL cryopumps were operational. The minimum base pressure was 9.9E-7 Torr-Kr with a pumping speed about 1.6 times VTF-2. The beam dump for this facility is made of graphite baffles angled about 30 degrees off the plane normal to the beam axis.

3. Controlling background pressure

In FIT 1, we operated the thruster at 3 different background pressures in VTF-2. This included the base operating pressure (i.e. the lowest achievable pressure when the thruster is operating at 4.5kW), as well as two and three times that pressure. We achieved the higher pressure conditions by introducing neutral krypton via a 1/4" Swagelock tubing with an elbow oriented downward 1.07m below and 1.78m downstream of the thruster. We replicated this study in LVTF at the same background pressures with the backflow positioned the same relative to the thruster as done in VTF-2. We included an additional low pressure condition in FIT 2 due to the higher pumping speed.

4. Electrical harnessing

We note in this section that the thruster harness can impact the time-varying thruster properties and thus the overall performance. We incorporated the same discharge filter design during both test campaigns. The filter is an RC circuit containing three parallel resistors for a total of 0.533 Ohms and a 100uF capacitor. The power supplies varied between facilities. In FIT 1, we used a Magna-Power Electronics supply rated to 20kW with a capacitance of 2115μF. In FIT 2, we used a Magna-Power Electronics supply rated to 150kW with a capacitance of 7800 μF. Additionally, the power lines differed in length and power ratings which could contribute to variability in the thruster impedance.

C. Diagnostics

We outline in the following the diagnostics we employed for the experimental campaigns. In order to reduce ambiguity about probe-related variances, we used in most cases the same physical probes in both test facilities.

1. Ion Gauge

We measured the background pressure with two 370 Stabil-Ion® Hot-cathode Ionization Vacuum Gauges. We mounted the ion gauge face to a KF elbow tube with a grid covering the front to neutralize ions entering. We placed a thermocouple on the mounting structure at the face of the gauge. We positioned the first (IG1) in the plane of the thruster and 1.75m off of centerline. To ensure we collected ambient neutrals, the gauge front faced towards the thruster. We positioned the second gauge (IG2) 1m behind the thruster facing away from the thruster. With the goal of matching pressures between facilities, we monitored and adjusted pressure based on IG1. To account for some of the thermal effects in the facility, we corrected the pressure from the gauge for temperature variance.[13] Figures 2a and 2b illustrate this set up.

We converted the expression for particle flux to terms of temperature using the ideal gas law and equation for kinetic energy:

$$nv = \frac{P}{k_B T}\sqrt{\frac{2k_B T}{M}} \propto \frac{P}{\sqrt{T}}, \tag{1}$$

(a)

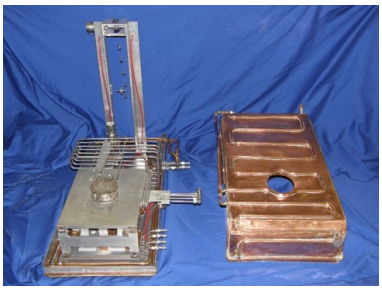

(b)

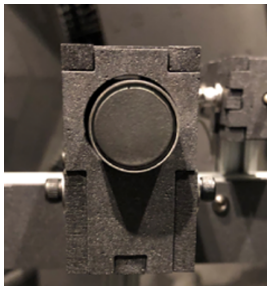

(c)

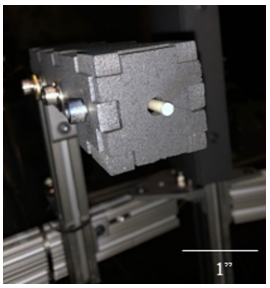

(d)

Figure 3: Images of the following diagnostics used in FIT 1 and FIT 2: a.) Ion gauge with a thermocouple, b.) GT thrust stand, c.) Faraday probe, and d.) Langmuir probe.

where n is the density, v is velocity, P is pressure, k_B is Boltzmann's constant, T is temperature, M is the mass of krypton. An image of the ion gauge set up in LVTF is provided in Figure 3a.

2. Thrust Stand

To measure performance, we utilized two thrust stands to measure the thrust at each background pressure. Both the GT and UM thrust stands are based on a null-type inverted pendulum design by NASA Glenn Research Center described in Refs. [14–16]. Each thrust stand was calibrated for measurements ranging from 110-450 mN in VTF-2 and 90-380 mN in LVTF. Both thrust stands were covered in a cooled copper shroud. From thrust measurements, we were able to calculate other performance metrics such as specific impulse and efficiency:

$$I_{sp} = \frac{T}{\dot{m}_p g_0} \qquad \eta = \frac{T^2}{2\dot{m}_p P_{in}}. \tag{2}$$

Here T is thrust, $\dot{m}_p$ is the total mass flow rate, g_0 is the acceleration of gravity, P_{in} is the input power.

3. High frequency current and voltage probes

To monitor the thruster current oscillations we positioned current probes on the cathode line between the chamber and discharge filter. We used different current probes at each facility on the cathode power line. For FIT 1 we set up a Teledyne LeCroy current probe. For FIT 2 we used a Tektronix current probe, since we did not have the proper equipment to read the DC component of the FIT 1 probe. We tested the AC component of the probes during FIT 2 and found them comparable. We also used sense lines to measure the discharge voltage oscillations and cathode-to-ground voltage oscillations. The voltage probes were the same at each facility, Powertek Differential Probes. We connected the probes to an oscilloscope. We implemented the same sample rate of 1MS/s and captured 100,000 samples at each pressure condition.

4. Faraday Probe

The Faraday probe used in this experiment was the same at the two facilities. It is a nude-type probe based on a JPL design.[17] We biased the Faraday probe guard and collector by -30V to collect only current in the ion saturation region. Using the probe dimensions, we calculated the ion current density from -90 to 90° across the thruster plume. We mounted the probe to a rotational stage 1 m from the thruster. We then calculated plume properties such as ion beam current, the portion of the discharge current carried by the ions, and the plume divergence, the spread of current off of the thrust axis.

The ion beam current equation is

$$I_B = 2\pi r^2 \int j(\theta) \sin\theta d\theta, \tag{3}$$

where j is the ion current density, $r = 1$m is the probe distance from the thruster, θ is the angular position of the probe. The divergence equation is

$$\cos\theta_d = \frac{2\pi r^2 \int j(\theta) \cos\theta \sin\theta d\theta}{I_B}. \tag{4}$$

5. Langmuir Probe

We characterized the behavior of the far-field plasma potential with respect to pressure with a Langmuir probe placed 1m from the thruster face and mounted on a rotational stage. The probe was a cylindrical design with tungsten wire. We biased the wire from -10V to 30V with respect to ground to determine the voltage at which the plasma potential exists.[18] From these measurements, we used it coupled with the cathode to ground potential to estimate the plasma to cathode potential, i.e. the "cathode coupling voltage."

III. Results

We tested the H9 at 300V 4.5kW in VTF-2 and LVTF on krypton. For the plume diagnostics and thrust measurements, we waited until the thruster reached thermal steady state at a predetermined 3 hours in both facilities. We also verified that the thruster reached thermal steady by monitoring a thermocouple attached to the thruster body. We noticed that the flow rate necessary to maintain 15A continued to increase until thermal steady state was achieved. We first present in the following the performance results at each facility. We then provide an overview results from plume measurements.

A. Pressure

We refer to the different background pressures in the folowing as P0.8x, P1x, P2x, and P3x. We show a table of these background operating pressures as well as the total thruster flow necessary to maintain 15 A discharge current in Table 1. We have normalized in this case the flow rates with respect to the LVTF P0.8x condition, which is the maximum flow recorded from both facility tests.

From this table we notice that the total flow rate decreases as pressure increases at each facility. This is due in part to the response to increased neutral ingestion with higher facility pressure.[2] We also show that ion gauge #2 changed nonlinearly compared to the pressure recorded at ion gauge #1 . This is an example of a difference between the facilities that could impact the comparison. Since pressures do not scale similarly at every position in the chamber. We plot this in Figure 4.

	IG1 Pressure	FIT 1 IG2 Pressure	FIT 1 Flow	FIT 2 IG2 Pressure	FIT 2 Flow
P0.8x	4.6μTorr			4.0μTorr	1.000
P1x	5.8μTorr	8.7μTorr	0.982	4.8μTorr	0.996
P2x	12.5μTorr	9.0μTorr	0.976	9.8μTorr	0.992
P3x	17.6μTorr	22.1μTorr	0.972	13.4μTorr	0.990

Table 1: Background pressures from the ion gauges and the associated total flow rates normalized when operating at constant power at each facility.

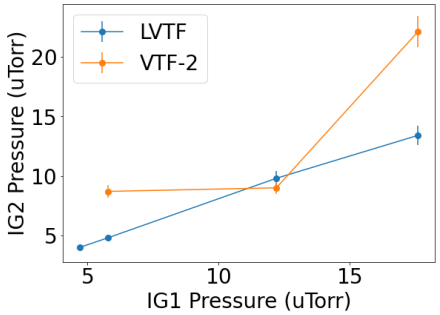

Figure 4: IG2 pressures with respect to IG1 with 6% uncertainty according to the manufacturer

B. Performance

We show a comparison of the global performance metrics in Figure 5. We evaluated these based on thrust measurements performed in the two facilities. The uncertainty incorporates the calibration uncertainty and the standard deviation of the measurement (two measurements per pressure in LVTF and three in VTF-2). The specific impulse and efficiency results are based on the relations shown in Eq 2.

As can be seen from these figures, the VTF-2 results demonstrate varying thrust, specific impulse, and efficiency with changing pressure, but no distinct trend outside of uncertainty. The LVTF results, on the other hand, exhibit a 4% increase in thrust (and corresponding variation in efficiency and specific impulse) as a function of the background pressure. These trends are statistically significant and outside the uncertainty estimates. This difference in trends is notable given that the pressure is matched, and we employed the same thruster.

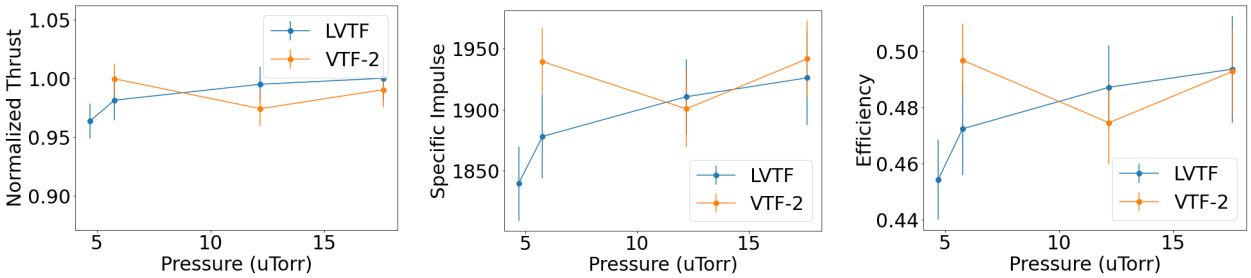

(a) (b) (c)

Figure 5: Performance results at each facility with respect to pressure for a.) Thrust normalized by the maximum value, b.) Specific impulse based on thrust and flow measurements, c.) Efficiency based on thrust and flow measurements.

C. Oscillations

This difference in facilities is also exhibited in the oscillation response, as can be seen in Fig. 7. In both test campaigns, the discharge oscillations did not experience any distinct changes with pressure variance. The breathing mode occurred for both facilities at about 17 kHz with relatively the same magnitude. This is within the range of frequencies typical for Hall thrusters.[19] For many thrusters, the breathing mode is a broad feature like the VTF-2 traces (Fig. 6a), but it is clear in the LVTF result (Fig. 6b). Interestingly, the LVTF result has a minute shift in the breathing mode frequency. The breathing mode frequency increased with pressure as response to the potential neutral ingestion impacting the rate of neutral depletion and resupply. The intensity of the mode remains constant. The VTF-2 result does not show this trend or it is unresolvable due to the small signal with respect to the other frequencies. Some devices will only experience a pressure response at certain power levels.[5] The largest peak for both tests is a cathode mode that varies in frequency and magnitude between facilities. This could be due to the cathode exchange or a slight change in

the positioning of the cathode. It could also be directly related to the electrical configuration with the facility or the cathode plume coupling to the plasma. Additionally, we note the presence of a potential harmonic of the cathode mode. Other key features include the divergence of the results at the higher frequencies. The additional modes in VTF-2 is not found in LVTF, but overall LVTF contains stronger oscillations at higher frequencies.

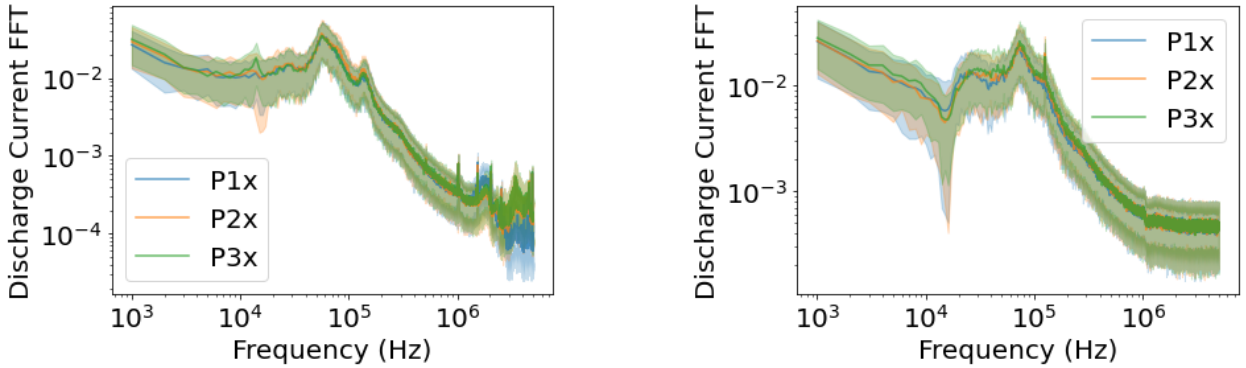

(a) (b)

Figure 6: Fast Fourier transform of the discharge current waveform with uncertainty at a.) VTF-2 and b.) LVTF.

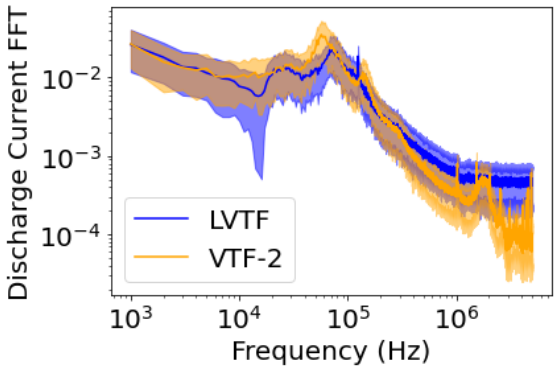

Figure 7: Fast Fourier transform of the discharge current waveform with uncertainty in VTF-2 and LVTF at P1x.

From these performance measurements, the thruster demonstrates contrasting trends in the pressure dependency. To further understand these results, we will present the plume measurements from the probe diagnostics.

D. Plume Measurements

We show in Figures 8a and 8b the ion current density collected as an average across two sweeps from -90° to 90° in the plume for both facilities as a function of facility pressure. We correct for the error that is due to the probe geometry for current can be captured in between the gaps of the probe guard and collector.[20]

The current traces in both facilities share qualitatively similar features. They are characterized by two peaks on centerline representative of the main discharge with an exponentially decreasing magnitude in current density at higher angles. We similarly see in both cases a marked increase in current density at more oblique angles. This trend is attributed to increased charge exchange collision and enhanced scattering of the thruster beam off ambient neutrals.[21]

While Fig. 8 shows qualitatively similar responses, we can see there are quantitative differences between the facilities with direct comparisons in Fig. 9. The LVTF profile is wider at higher angles than the VTF-2

profile. There is also less current along channel centerline in the LVTF result. This is consistent for P2x and P3x. Physically, these results suggest that the Hall thruster plume at all pressures is effectively more divergent in LVTF. We note that there is closest agreement at P3x.

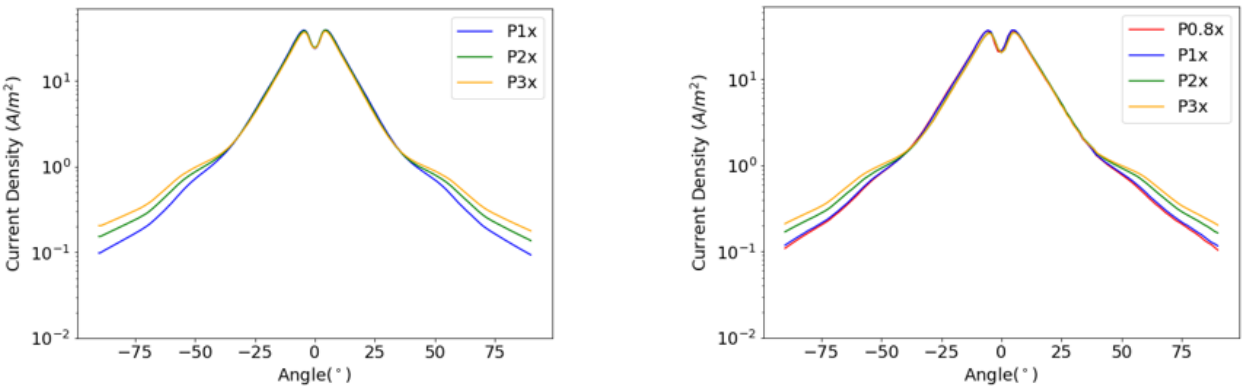

(a) (b)

Figure 8: Plots of the current density profiles in log scale from -90° to 90° as a function of pressure in a.) VTF-2 and b.) LVTF.

As another point of comparison between the facilities, we examine the plasma potential as a function of position 1 m from the thruster and referenced with respect to the cathode. This is also the cathode coupling voltage, which has been documented to change with background pressure.[22] In Figures 10a and 10b, we plot the plasma potential at various angular positions across the plume for the three background pressure conditions. We see that the profiles exhibit a peak near centerline, consistent with the increase in plasma density near the thruster centerline. The magnitude of plasma potential profiles increases with respect to pressure. This qualitatively suggests electrons require a stronger bias to couple to the plume. We capture this trend more quantitatively by showing showing an average for the plasma potential over all positions as a function of pressure in Fig. 11b. As discussed in Ref. 22, Jorns and Byrne showed that the coupling voltage can exhibit different dependencies with pressure depending on the mechanism dominating the local plume. Following this previous work, our results would suggest that for both VTF-2 and LVTF, a Boltzmann effect is dominating the local plume dynamics' response to facility pressure.

Significantly, we note here that in a departure from the Faraday and global plume measurements, the trends in plasma potential are within uncertainty for both facilities. This suggests that at least per this metric, the near-field electron coupling dynamics are similar.

E. Efficiency Modes

With the previous current density results we can perform an analysis of select efficiency modes for the thruster. We motivate these via the model presented in Refs. 23, 24 for the anode efficiency:

$$\eta_a = \eta_b \eta_m \eta_d \eta_q \eta_v. \tag{5}$$

Here we have the beam utilization, mass utilization, divergence, charge utilization, and voltage utilization efficiencies, in order listed. This model provides insight into the underlying physical processes driving the response of the thruster in each facility to background pressure.

In this work, we only consider the first three efficiency modes in Eq. 5 as we did not have the diagnostics to evaluate the latter contributions in both test campaigns. To solve for the efficiency modes, we utilized the parameters calculated from Faraday probe data, beam current and divergence described in Section 2.[24] These parameters directly relate to the specific Hall thruster efficiencies we analyzed. The beam utilization efficiency is

$$\eta_b = I_B / I_D, \tag{6}$$

where I_D is the discharge current. The beam utilization efficiency describes how much of ion current contributes to the discharge current instead of electron current ($I_D = I_B + I_e$). With the beam current we

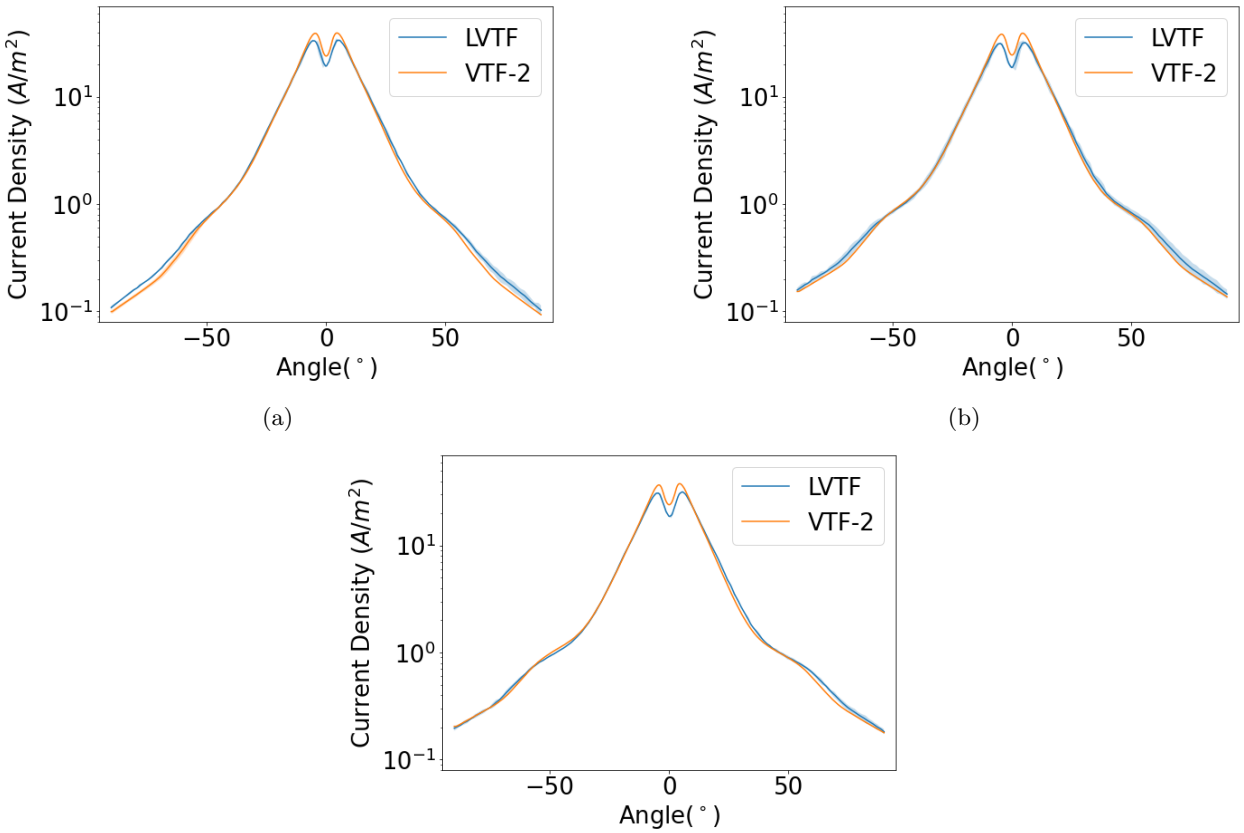

(a)

(b)

(c)

Figure 9: Plots of the current density profiles in log scale from -90° to 90° in each facility with 3σ uncertainty bands at a.) P1x b.) P2x and c.) P3x.

can also calculate an approximation for the mass utilization efficiency, as well, which describes how much of the flow is converted to current carrying ions. This is expressed by the relationship:

$$\eta_m = \frac{\dot{m}_i}{\dot{m}_a} \propto \frac{I_b}{\dot{m}_a}, \tag{7}$$

where $\dot{m}_i$ and $\dot{m}_a$ are the ion mass flow rate and anode flow rate. This efficiency mode represents the thruster's ability to convert propellant neutrals to ions. This equation does not account for the current carried by multiply charged species which will decrease the mass utilization efficiency. This is typically found using a different diagnostic, an ExB analyzer, that was not included in this campaign. Lastly, we can express the divergence efficiency as

$$\eta_d = \cos^2(\theta_d). \tag{8}$$

The divergence efficiency represents how much of the plume is directed axially and contributes to thrust.

We note here that to estimate these plume parameters and efficiencies from our measured Faraday traces, we must account for the impact of charge exchange ions. This artificially skews the current collected by the probe, widening it, and thus must be deconvolved from the trace. We do so by performing an average of various previously demonstrated techniques- a flat subtraction of the minimum current density, an exponential fit, and a Gaussian fit.[20,25–28] In our following results, we present the average results from applying these three techniques to the current density profile. The uncertainty in the values reflects the variance across these correction methods.

With this in mind, we show in Fig. 12a the results as a function of pressure of beam utilization, mass utilization, and divergence efficiency for both facilities. We first note the beam utilization increases suggesting that higher pressure results in a larger fraction of the total discharge current being carried by the ion beam

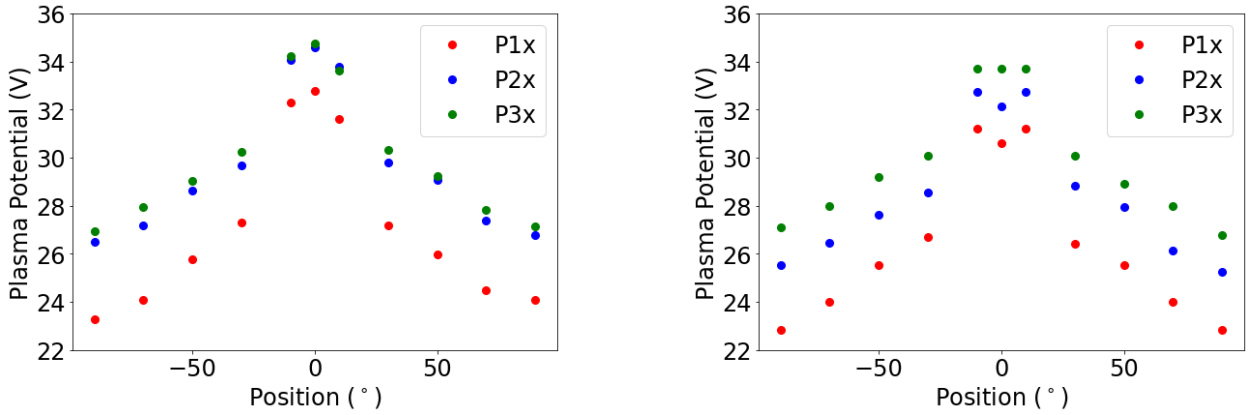

Figure 10: A plot of the plasma potential as a function of background pressure in a.) VTF-2 and b.) LVTF.

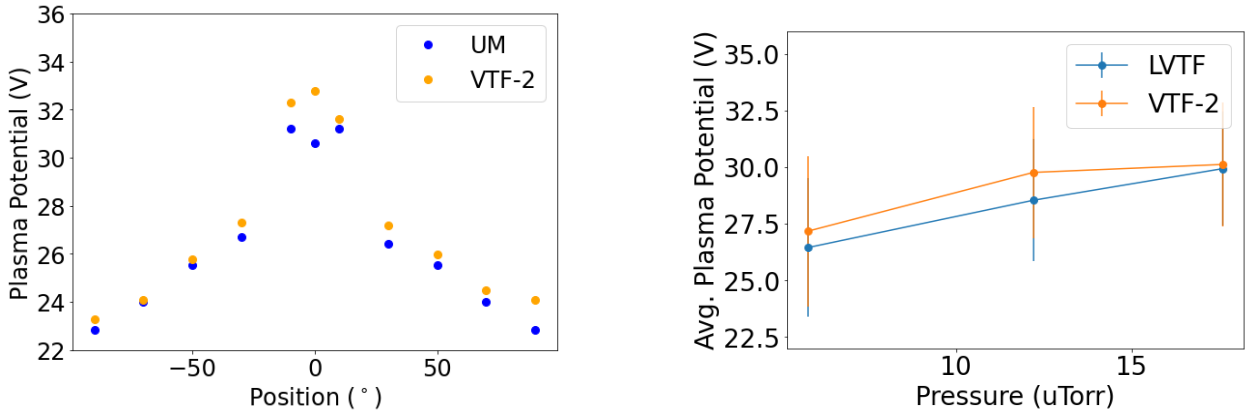

Figure 11: a.) A plot of the plasma potential in each facility at P1x. b.) A plot of the average plasma potential in each facility with varying background pressure.

instead of the electrons. This directly relates to the electron confinement in the Hall thruster channel, higher pressure improves electron confinement. The beam utilization in VTF-2 is lower than in LVTF.

As shown in Fig.12a, the mass utilization trends upward as well with facility pressure. This effect has in part been attributed to higher neutral density ingestion and has been observed across a wide variety of Hall thruster designs.[1,2,4–6,9,27] As with the beam utilization, the estimate for mass utilization is higher and outside of uncertainty bars for the LVTF results compared to VTF-2. This indicates that LVTF more efficiently converts neutrals to ions.

Finally, we note the divergence efficiency also increases with pressure as well. This trend has been noted for a variety of various Hall thruster studies.[4–6,9,27] This physically has been attributed in part to the fact that the acceleration region in the thruster shifts upstream with increasing pressure resulting in a more collimated beam. Ions are accelerated deeper into the channel where strong axial electric field components are present.[7,8,29] Unlike the other two efficiency modes, we note that the LVTF result is more divergent than the VTF-2 results.

In summary, with these findings, we show an overall increase in three of the efficiency modes with this pressure. This is in contrast to the global efficiency (Fig. 5c). Notably, we would expect the product of these three trends to scale with the overall efficiency results (Fig. 12b). This is in fact the case for the LVTF results, but as discussed in the previous section, VTF-2 results for overall efficiency do not change outside

of the uncertainty estimates. Relatedly, if we consider the products of the efficiency modes and compare these to the measurement, the LVTF-2 probe data is generally consistent in magnitude with the measured data (allowing for the fact that the other efficiency modes will raise the product efficiency estimate). The product of the efficiency modes for the VTF-2 results markedly underestimates the measured efficiency. These inconsistencies ultimately may point to the role of missing efficiency modes or possibly errors in the thrust or probe measurements. Different thrust stands were used or the probes may have been angled off axis when mounting. We expand on the discrepancies in the next section.

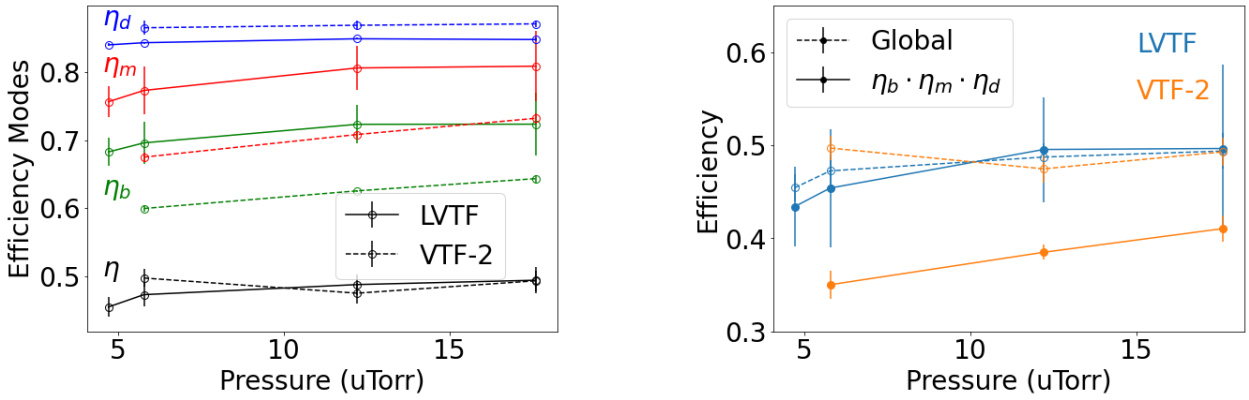

(a) (b)

Figure 12: A plot of a.) the total efficiency and the efficiency modes and b.) the product of the available efficiency modes as a function of pressure at each facility.

IV. Discussion

In this section we comment in detail on the implications of our findings in the context of the different responses exhibited in the facilities.

A. Efficiency mode variation due to charge exchange correction

We first will investigate the efficiency mode findings. To calculate the efficiency modes, it is necessary to account for the charge exchange effect in the current density measurements. We previously mentioned doing so by averaging various methods implemented in the community. These include subtracting the current density trace by the minimum at 90 degrees assuming the current in that region is solely charge exchange ions.[25] We also fit a portion of the profile to a Gaussian curve, as well as an exponential curve.[20,27] Upon further inspection, it seems that the curve fitting procedures may be removing key features in the wings of the profile causing an over-correction for charge exchange. We will note here that the suggested Gaussian and exponential curves have successfully corrected for charge exchange in Hall thruster current density profiles with less prominent features than seen in these results. It could be that the corrections are not appropriate for the profiles in this work. With that, we show the results of the efficiency modes, as well as the product of the available modes when using solely the subtraction method in Fig. 13. We notice that the trends between the facilities now agree more closely. Yet, the trends decrease with higher pressure. For divergence specifically, this disagrees with the typical Hall thruster pressure dependence.[6] Additionally, there are larger deviations for the LVTF result when the product of the available modes are compared to the global efficiency. The VTF-2 results are closer in magnitude, but the trends do not agree overall. These results demonstrate a need for more investigation in the charge exchange corrections for this variant of Hall thruster plume.

B. Decrease in performance with lower facility pressure compared to other Hall thrusters with center-mounted cathodes

As we have discussed in the preceding, the H9's global performance metrics in LVTF and its efficiency modes in both LVTF and VTF-2 exhibited a decrease with lower facility pressure. This result is counter to previous

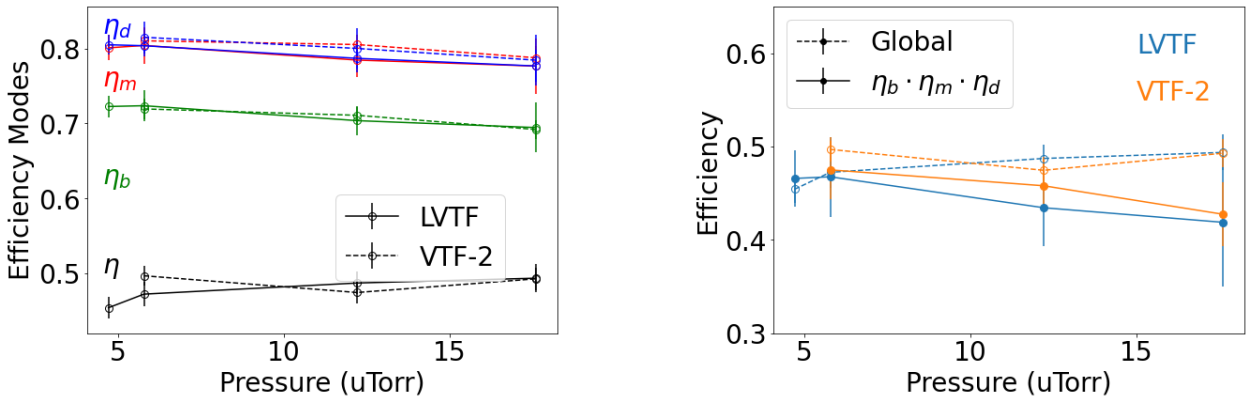

(a) (b)

Figure 13: A plot of a.) the total efficiency and the efficiency modes and b.) the product of the available efficiency modes as a function of pressure at each facility using a flat subtraction to correct for charge exchange.

parametric pressure based studies that have been performed on thrusters with center-mounted cathodes like the HERMeS thruster.[6] In some cases, the insensitivity to pressure has in part been attributed to the fact that the center-mounted cathode is a large source of neutral flow, therefore masking the relatively small impact of neutral density changes attributed to the increase in background pressure.

As the physical mechanisms causing the changes in plasma properties with facility pressure remain poorly understood, we cannot directly comment on why the H9 in this case exhibits different behavior. With that said, we do note one notable change in these previous campaigns, that is we employed krypton as the operating propellant. As Fig. 12 shows, krypton operation is lower than typical xenon performance with lower mass utilization efficiency. This qualitatively suggests that changes in neutral ingestion may have a more pronounced impact on features. Indeed, as was shown in the work of Su and Hurley,[30,31] flow rates are a critical factor in impacting the mass utilization of the system.

In light of this possible explanation, these studies performed on the H9 and across the facilities are not a broad representation of the previous decade of work performed on facility response with xenon-fed Hall thrusters.

C. Nature of difference in facility response

We have noted in the preceding that to first order, it is unexpected that the results in the facilities should disagree with pressure. We have attempted to ensure consistency between the test campaigns including adopting the same convention for elevating the facility pressure and measuring it. The disparity, provided it is outside error bars, invites a few possibilities we consider here: 1) that the thruster configuration may have changed between tests or 2) that using the facility pressure measured at one location is not sufficient for ensuring the facility background pressure configurations are the same.

1. Quantifying differences in thruster configuration

In order to assess our first hypothesis, we need a way to attempt to de-convolve the pressure effects to allow for a direct comparison of thruster configuration in the two facilities. To this end, we adopted Brown et al[20] first-order method to extrapolate the current density profiles from both facilities to a "zero background pressure" condition. This method is based on applying a linear extrapolation of the current density with respect to pressure at each angular position. We show examples of this in Figure 14a drawn from our experimental plume profile.

We conducted this extrapolation at both facilities where we show the results in Figure 14b. As can be seen, the profiles ultimately differ with the extrapolated pressure conditions from LVTF exhibiting a more divergent profile. Intuitively, if the thruster configuration were the same, we would expect these extrapolated profiles to match, regardless of the response of the thruster at higher pressure. This result thus supports

the idea that the thrusters may have a fundamental difference in configuration. While it is unlikely such a difference could be attributed to changes in the thruster build or geometry, which was verified between tests, there are other aspects of the facility environment that could be contributing factors. For example, the electrical configuration of the facilities as represented by the proximity of conducting surfaces and beam dump placement were different. The role these effects may have to play on thruster operation for the H9 have yet to be fully evaluated but are the subject of on-going investigation.[32]

As a caveat to this discussion, we remark there are also limitations to this approach to extrapolation as well. Most notably, it is based on the assumption that there is a linear scaling between our single point measurement of the near-field pressure and the local neutral density at each measurement location in the plume. As shown in Fig. 8, this is not always the case. This observation invites the possibility that there may be two-dimensional effects in the background pressure precluding a direct linear extrapolation to zero. We expand on this possibility in the next section.

2. Challenges in ensuring parity in background pressure between facilities

While we matched in this study the facility pressures with a single pressure gauge, IG1, we recognize it is possible this does not ensure that the near-field pressure the thruster plane is the same between facilities (see Fig. 4). Given that this is the most critical factor in driving the internal plasma dynamics such as divergence, mass utilization, and beam utilization, such a difference could in part explain the preceding results. To this point, qualitatively, our results might suggest that the near field neutral density in LVTF is lower than that for the VTF-2 results. This stems primarily from the fact that the mass flow rates from the anode in order to maintain the same current in the LVTF configuration were higher, suggesting that there is less ambient flow from the facility to augment the discharge current.

This possibility invites the question as to whether there is a metric available to perform a more direct comparison of facility neutral pressures. The anode mass flow rate may be an appropriate proxy. Intuitively, the variation in this parameter accounts for the variation in the neutral density in the near-field. A larger variation in this parameter compared to a reference point is indicative of an increased background neutral effect.

Proceeding under this assumption, we show in Fig. 16 the global performance metrics as a function of the normalized change in anode mass flow rate compared to the maximum anode flow rate (lowest pressure condition for LVTF). As can be seen, these results qualitatively allow the global performance metrics to follow a consistent trend. Physically, this result may suggest that the near-field neutral density for VTF-2 is higher than the LVTF for a given measured pressure at the IG1 location. This underscores the need potentially to identify a more rigorous standard for comparing pressure response across facilities, adopting, for example a metric such as this change in mass flow rate.

With that said, we caveat this result with a comparison of the efficiency modes (divergence, mass utilization, and beam utilization) as a function of the change in anode mass flow rate in Fig. 16c, which shows an evident discontinuity between the facilities for two of the efficiency modes. The one exception is divergence, which is consistent with the global trends. As discussed in the preceding, this may be an artifact of systematic error in the analysis of the results. It also may point to a fundamental drawback of electing this parameter as a proxy for the background pressure effects. Indeed, in light of this limitation, there is a need to explore and identify other possible metrics for background pressure to ensure equivalence across facilities.

V. Conclusion

The goal of this work has been to compare the performance of a Hall effect thruster in different facilities as a function of facility background pressure. To this end, we have attempted to replicate and extend a pressure study on the H9 Hall effect thruster at a fixed operating condition with krypton propellant across two facilities- VTF-2 and LVTF. Despite implementing the same thruster, filter, and diagnostics, we ultimately found that the thruster's response to facility pressure varied between facilities. Thruster global performance metrics such as thrust, efficiency, and specific impulse as well as select plume characteristics differed both in magnitude and overall trends with facility pressure. For the LVTF facility, there was overall a general decrease in performance with lower facility pressure, while the overall efficiency in VTF-2 remained invariant to background pressure. Notably, the efficiency modes of the thruster in both facilities mirrored the trends in global performance exhibited in LVTF and not VTF-2.

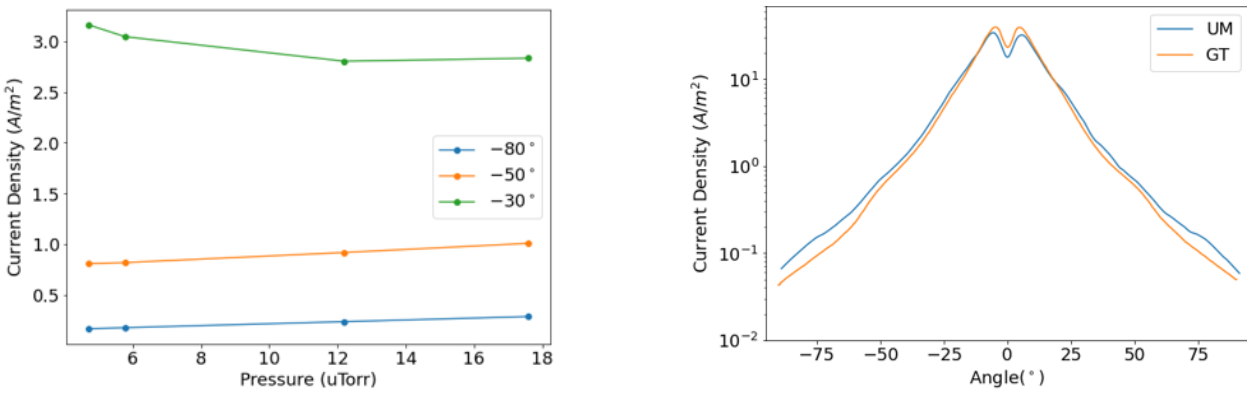

(a) (b)

Figure 14: a.) Fit procedure for linear extrapolation to b.) the current density at P0x

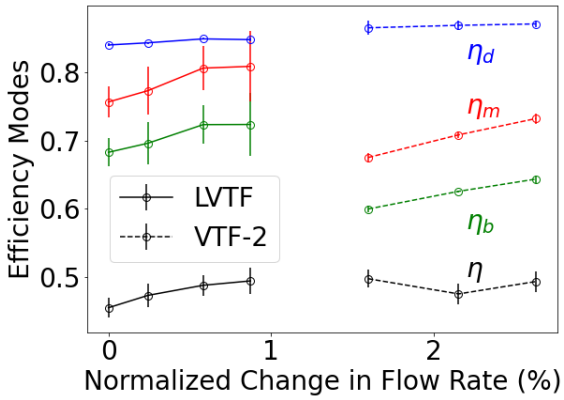

Figure 15: A plot of the total efficiency and the efficiency modes with respect to the change in flow normalized by the maximum flow rate.

In light of these findings, we have discussed different hypotheses to discuss the differences exhibited in the two facilities. Key explanations include the existence of systematic errors in one or both campaigns, that the variation results from other differences in the facility configuration, e.g. electrical boundary conditions, that drive this effect, that there are issues or that the single point measurement we have used for background pressure is an inadequate proxy for the near-field neutral density in both facilities. To explore this last trend, we have shown that the necessary change in flow rate to maintain a constant current may be a more appropriate standard to compare the results. This motivates the need to investigate this metric as well as others for standards to match facilities when performing pressure studies.

In summary, these findings are an additional contribution to the larger community for helping identify standards when performing Hall thruster pressure studies. These studies similarly are integral to JANUS as they provide the necessary dataset for refining and regressing models capable of extrapolating between facilities and ultimately to orbital conditions.

Acknowledgments

The authors would like to thank the NASA Space Technology Research Opportunity, Grant 80NSSC22K1172, as well as the NASA Research Institute, the Joint AdvaNced propUlsion inStitute (JANUS), for supporting this work. The authors would also like to thank those that supported testing Miron Liu, Declan Brick, John Riley O'Toole, and the HPEPL team.

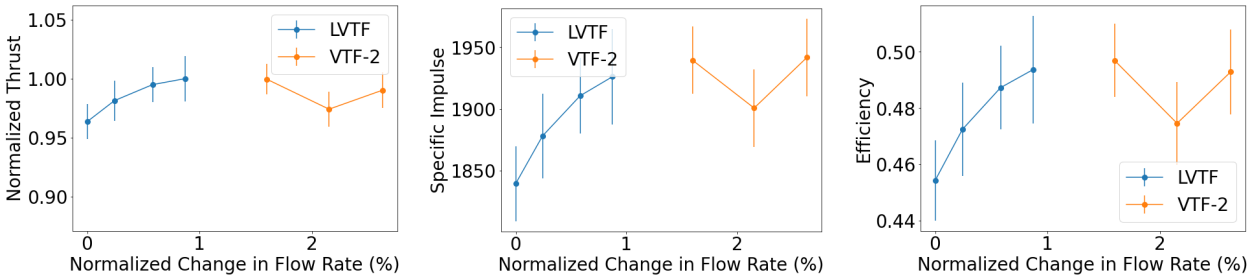

(a) (b) (c)

Figure 16: Performance results at each facility with respect to the change in flow normalized by the maximum flow rate for a.) Thrust normalized by the maximum value, b.) Specific impulse, and c.) Efficiency .

References

[1]Randolph, T., Kim, V., Kaufman, H., Kozubsky, K., Zhurin, V., and Day, M., "Facility Effects on Stationary Plasma Thruster Testing," *Proceedings of the 23rd International Electric Propulsion Conference*, 1993.

[2]Hofer, R. R., Peterson, P., and Gallimore, A., "Characterizing Vacuum Facility Backpressure Effects on the Performance of a Hall Thruster," *27th International Electric Propulsion Conference*, 2001, pp. IEPC–01–045.

[3]Byers, D. and Dankanich, J., "A Review of Facility Effects on Hall Effect Thrusters," *31st International Electric Propulsion Conference*, 2009.

[4]Diamant, K. D., Liang, R., and Corey, R. L., "The Effect of Background Pressure on SPT-100 Hall Thruster Performance," *50th AIAA/ASME/SAE/ASEE Joint Propulsion Conference*, American Institute of Aeronautics and Astronautics, 7 2014.

[5]Huang, W., Kamhawi, H., Lobbia, R. B., and Brown, D. L., "Effect of background pressure on the plasma oscillation characteristics of the HiVHAc Hall thruster," *50th AIAA/ASME/SAE/ASEE Joint Propulsion Conference 2014*, 2014, pp. 1–14.

[6]Huang, W., Kamhawi, H., Haag, T. W., Ortega, A. L., and Mikellides, I. G., "Facility effect characterization test of NASA's HERMeS hall thruster," *52nd AIAA/SAE/ASEE Joint Propulsion Conference, 2016*, Vol. AIAA-2016-, 2016.

[7]MacDonald-Tenenbaum, N., Pratt, Q., Nakles, M., Pilgram, N., Holmes, M., and Hargus, W., "Background pressure effects on ion velocity distributions in an spt-100 hall thruster," *Journal of Propulsion and Power*, Vol. 35, 2019, pp. 403–412.

[8]Cusson, S. E., Dale, E. T., Jorns, B. A., and Gallimore, A. D., "Acceleration Region Dynamics in a Magnetically Shielded Hall Thruster," *Physics of Plasmas*, Vol. 26, 2019.

[9]Huang, W. and Kamhawi, H., "Facility Effects on the Ion Characteristics of a 12.5-Kilowatt Hall Thruster," *Journal of Propulsion and Power*, 3 2023, pp. 1–10.

[10]Eckels, J., Marks, T., Allen, M., Jorns, B., and Gorodetsky, A., "Hall thruster model improvement by multidisciplinary uncertainty quantification," *Journal of Electric Propulsion*, Vol. 3, 9 2024, pp. 19.

[11]Hofer, R. R., Cusson, S. E., Lobbia, R. B., and Gallimore, A. D., "The H9 Magnetically Shielded Hall Thruster," *35th International Electric Propulsion Conference*, 2017, p. 232.

[12]Cusson, S. E., Hofer, R., Lobbia, R. B., Jorns, B. A., and Gallimore, A. D., "Performance of the H9 Magnetically Shielded Hall Thrusters," *35th International Electric Propulsion Conference*, 2017, p. 239.

[13]Dankanich, J. W., Walker, M., Swiatek, M. W., and Yim, J. T., "Recommended Practice for Pressure Measurement and Calculation of Effective Pumping Speed in Electric Propulsion Testing," *Journal of Propulsion and Power*, Vol. 33, 5 2017, pp. 668–680.

[14]Haag, T. W., "Thrust stand for high-power electric propulsion devices," *Review of Scientific Instruments*, Vol. 62, 5 1991, pp. 1186–1191.

[15]Xu, K. G. and Walker, M. L. R., "High-power, null-type, inverted pendulum thrust stand," *Review of Scientific Instruments*, Vol. 80, 5 2009.

[16]Polk, J. E., Pancotti, A., Haag, T., King, S., Walker, M., Blakely, J., and Ziemer, J., "Recommended Practice for Thrust Measurement in Electric Propulsion Testing," *Journal of Propulsion and Power*, Vol. 33, 5 2017, pp. 539–555.

[17]Walker, M., Hofer, R., and Gallimore, A., "The Effects of Nude Faraday Probe Design and Vacuum Facility Backpressure on the Measured Ion Current Density Profile of Hall Thruster Plumes," *38th AIAA/ASME/SAE/ASEE Joint Propulsion Conference & Exhibit*, American Institute of Aeronautics and Astronautics, 7 2002.

[18]Lobbia, R. B. and Beal, B. E., "Recommended Practice for Use of Langmuir Probes in Electric Propulsion Testing," *Journal of Propulsion and Power*, Vol. 33, 5 2017, pp. 566–581.

[19]Choueiri, E. Y., "Plasma oscillations in Hall thrusters," *Physics of Plasmas*, Vol. 8, 4 2001, pp. 1411–1426.

[20]Brown, D. L., Walker, M. L. R., Szabo, J., Huang, W., and Foster, J. E., "Recommended Practice for Use of Faraday Probes in Electric Propulsion Testing," *Journal of Propulsion and Power*, Vol. 33, 5 2017, pp. 582–613.

[21]Katz, I., Jongeward, G., Davis, V., Mandell, M., Mikellides, I., Dressler, R., Boyd, I., Kannenberg, K., Pollard, J., and King, D., "A Hall effect thruster plume model including large-angle elastic scattering," *37th Joint Propulsion Conference and Exhibit*, American Institute of Aeronautics and Astronautics, 7 2001.

[22]Jorns, B. A. and Byrne, M., "Model for the dependence of cathode coupling voltage in a hall thruster on facility pressure," *Plasma Sources Science and Technology*, 2020.

[23]Goebel, D. M. and Katz, I., *Fundamentals of Electric Propulsion*, Wiley, 10 2008.

[24]Hofer, R. and Gallimore, A., "Efficiency Analysis of a High-Specific Impulse Hall Thruster," *40th AIAA/ASME/SAE/ASEE Joint Propulsion Conference and Exhibit*, American Institute of Aeronautics and Astronautics, 7 2004.

[25]Hofer, R. R. and Gallimore, A. D., "Recent Results From Internal and Very-Near-Field Plasma Diagnostics of a High Specific Impulse Hall Thruster," *28th International Electric Propulsion Conference*, 2003, p. 037.

[26]Huang, W., Shastry, R., Herman, D., Soulas, G., and Kamhawi, H., "Ion Current Density Study of the NASA-300M and NASA-457Mv2 Hall Thrusters," *48th AIAA/ASME/SAE/ASEE Joint Propulsion Conference & Exhibit*, American Institute of Aeronautics and Astronautics, 7 2012.

[27]Huang, W., Kamhawi, H., and Haag, T., "Effect of Background Pressure on the Performance and Plume of the HiVHAc Hall Thruster," *33rd International Electric Propulsion Conference*, 2013, pp. IEPC–2013–058.

[28]Huang, W., Shastry, R., Herman, D. A., Soulas, G. C., and Kamhawi, H., "A New Method for Analyzing Near-Field Faraday Probe Data of Hall Thrusters," *49th AIAA/ASME/SAE/ASEE Joint Propulsion Conference*, American Institute of Aeronautics and Astronautics, 7 2013.

[29]Huang, W., Frieman, J. D., Kamhawi, H., Peterson, P. Y., Hofer, R. R., Branch, N. A., and Dao, H., "Ion Velocity Characterization of the 12.5-kW Advanced Electric Propulsion System Engineering Hall Thruster," *AIAA Propulsion and Energy 2021 Forum*, American Institute of Aeronautics and Astronautics, 8 2021.

[30]Su, L. L., Roberts, P. J., Gill, T. M., Hurley, W. J., Marks, T. A., Sercel, C. L., Allen, M. G., Whittaker, C. B., Viges, E., and Jorns, B. A., "High-Current Density Performance of a Magnetically Shielded Hall Thruster," *Journal of Propulsion and Power*, Vol. 40, 9 2024, pp. 729–746.

[31]Hurley, W. J. and Jorns, B. A., "Mass utilization scaling with propellant type on a magnetically shielded Hall thruster," *Plasma Sources Science and Technology*, Vol. 34, 5 2025, pp. 055010.

[32]Jovel, D. R., Cabrera, J. D., and Walker, M. L. R., "Hall effect thruster impedance characterization in ground-based vacuum test facilities," *Journal of Electric Propulsion*, Vol. 3, 12 2024, pp. 31.